Fiber Spinning of Viscoelastic Liquid

The fiber spinning process of viscoelastic liquid is successfully analyzed by means of a nonlinear integral constitutive equation, finite-element discretization, and Newton iteration. The process is cast and studied both as an initial value problem, which requires the specification of the drawing force, and as a two-point boundary value problem, which requires the specification of the draw ratio. Solutions are obtained up to high elasticity, high draw ratio, and large drawing force. The results agree with the analytic asymptotic solution for Newtonian liquid, with existing numerical solutions in the limiting case of the upper-convected Maxwell liquid, and with available experimental data on spinning of polystyrene melt at 170°C and low-density polyethylene at 150°C.

T. C. Papanastasiou, C. W. Macosko, and L. E. Scriven
Department of Chemical Engineering and Materials Science
University of Minnesota
Minneapolis, MN 55455

Zhao Chen
Macromolecular Research Center
University of Michigan
Ann Arbor, MI 48109

Introduction

Extrusion of polymer melts and solutions through orifice or slit dies to form fibers or sheets is common in many large-scale industrial applications such as fiber spinning, sheet casting, curtain coating, and others. Besides its use in production, the fiber-spinning technique is extensively employed as an extensional rheometer (Spearot and Metzner, 1972; Zeichner, 1973; Ferguson and Missaghi, 1974; Mewis and Gleyn, 1982), its advantages being the generation of high extension rates within liquids of low to high zero shear viscosity.

The constitutive equation used to describe the rheological behavior of a viscoelastic liquid is the prime ingredient of any analysis of how the liquid flows. Until now, differential constitutive models have been used commonly, but they are not very accurate in the sense that they fail to predict satisfactorily some of the elementary responses in standard rheological tests. Integral constitutive models have not been used extensively to analyze fiber spinning although in most cases they do predict the responses in standard rheological tests.

An associated difficulty in numerical modeling with differential constitutive models is the necessity of imposing essential boundary conditions on the viscous stresses at a synthetic inlet plane, because the exact value of these stresses is not known *a priori* at any section downstream of the die. This problem does not arise with Newtonian liquids, because the viscous stresses are explicitly related to velocity gradients; nor does it arise with integral constitutive models, because they demand instead a natural condition on the history of the deformation.

Matovich and Pearson (1969) studied the spinning of fibers of Newtonian, shear-thinning, and second-order fluids. The Newtonian and shear-thinning constitutive models accurately predicted the downstream behavior of inelastic fibers. The second-order fluid however, failed to describe even qualitatively the observed behavior of polymeric liquids.

Denn et al. (1975) and Fisher and Denn (1976) modeled the same process with generalized upper-convected Maxwell constitutive equations. The analysis showed that for a given elasticity there is a maximum attainable draw ratio at which the stresses are required to become infinite and processing is not possible. In their analysis the inflow velocity, the viscous stress at the inlet, and the drawing force are set and the draw ratio is estimated, whereas in practice the opposite is true: the desired fiber diameter and thus the draw ratio are set and these uniquely determine the required drawing force. Their formulation of the process as an initial value problem demands that the ratio of radial to axial stress be specified at the inlet. They assumed this ratio to be vanishingly small, and the results of their analysis proved to be insensitive to this ratio. To validate this assumption Keunings et al. (1983) analyzed the profile development in continuous drawing and found that for an upper-convected Maxwell model and the Phan-Thien and Tanner model (1977) this ratio lies between -0.5 and 0. Whether it does so for other models and what values it takes at high elasticity have not been examined. Thus the question of the stress boundary condition, or initial condition at the inlet remains open.

Recently Phan-Thien (1978) used a modified Phan-Thien and Tanner differential constitutive equation that accounts for multiple relaxation times and for elementary responses in shear and uniaxial elongation tests. His predictions with this spectrum of relaxation modes agreed with experimental data on spinning of low density polyethylene (Spearot and Metzner, 1972) and polystyrene (Zeichner 1973) melts. Although for the cases studied the equation behaved quite satisfactorily, some observations

Correspondence concerning this paper should be addressed to T. C. Papanastasiou, Department of Chemical Engineering, The University of Michigan, Ann Arbor, MI 48109.

are in order. To our knowledge the equation has not been evaluated in biaxial extension, the third fundamental mode of deformation. It appears to violate the fundamental Lodge-Meissner relation in stress relaxation (Lodge; 1975). The problem of the inlet stress may get worse because a stress value is required for each of the relaxation modes. Finally like earlier analyses, Phan-Thien's analysis requires specification of the drawing force, whereas in practice the draw ratio is specified.

Malkus (1981) studied isothermal fiber spinning as described by an integral model of upper convected Maxwell model-type by means of collocation finite element and functional Newton iteration. He found that the quadratic rate of convergence deteriorates near Deborah number one (maximum extension rate times relaxation time), beyond which the iteration fails to converge at all. Larson (1983) studied the same process as described by the Doi-Edwards (1979) model. He made use of an indirect solver based on an explicit finite difference scheme. His predictions with the Doi-Edwards model are similar to those of a corotational Maxwell liquid, but his algorithm failed to converge at drawing speeds lower than those achieved with the upper-convected Maxwell model.

In this paper we present an analysis with a nonlinear integral constitutive equation advanced by Papanastasiou et al. (1983). This equation was tested successfully in a wide spectrum of shear and elongational flows. These flows included:

- Transient and steady shear of two different polydimethlsiloxanes, a polyethylene, and a polystyrene
- Transient uniaxial elongation of a polyethylene and polystyrene
- Transient and steady biaxial extension of two different polydimethylsiloxanes and a polystyrene.

These results and the molecular characteristics of each of the melts are detailed in Papanastasiou et al. (1983). To our knowledge none of the employed differential constitutive equations had ever been tested successfully in such a broad spectrum of experimental data. The accurate predictions in transient elongational flows make the nonlinear integral constitutive equation particularly attractive for the analysis of the fiber spinning process. The resulting set of nonlinear algebraic equations is solved by full Newton iteration. A particular extensional prehistory is assumed; however, the analysis can easily be extended to other admissible prehistories, as is demonstrated below. Although a particular integral model is used here, the analysis that follows applies directly to all the other integral constitutive equations of the Bernstein-Kearsley-Zapas, or BKZ type (Bernstein et al., 1963) that have been put forward, including those developed recently from molecular theory (Doi and Edwards, 1979; Curtiss and Bird, 1981). In both analyses the equation set is solved either with a draw ratio boundary condition at the downstream end of the fiber or with a drawing force or tension boundary condition there.

Governing Equations

The fiber spinning process is shown schematically in Figure 1. An axisymmetric stream of viscoelastic liquid emerging from a hole of diameter D is taken up at position L downstream by a drawing force F at a speed u_L that is greater than the extrusion velocity. The extruded fiber initially swells owing to the relaxation of the normal stresses, but beyond a distance approximately two diameters downstream it slims continually. At or near the location of the maximum diameter, the axial velocity and the viscoelastic stress became virtually uniform over the cross section of the fiber, i.e., the flow becomes fully developed there. If the fiber is long enough, i.e., $L/D \gg 1$, the die-swell phenomenon becomes unimportant and the fiber diameter, drawing force, and draw ratio can be deduced by analyzing the flow between $0 \le z \le L$ as shown in Figure 1.

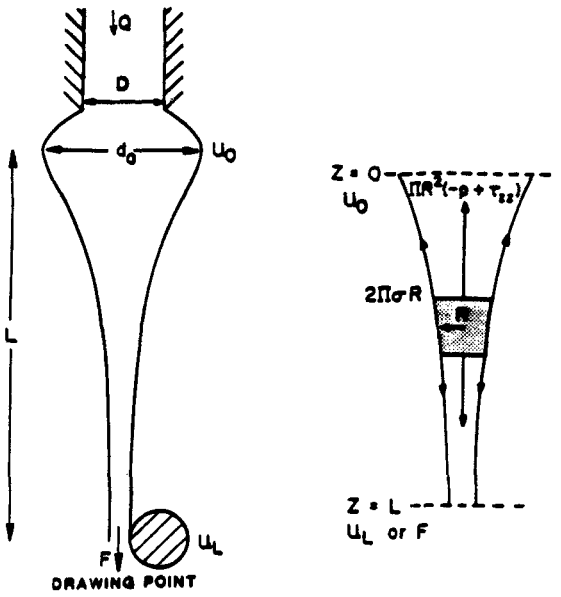

Figure 1. Fiber spinning process.
Axisymmetric stream emerges from a hole of diameter D with average velocity u_o. It is taken up at location L downstream by drawing force F at a speed of $u_L > u_o$. Liquid between $z = 0$ and $z = L$ is accelerated by viscous $[\pi R^2(p + \tau_{zz})]$, gravity $(\rho\pi R^2\, dz)$, and capillary $(2\pi\sigma R)$ forces.

Governing equations

The liquid between $z = 0$ and $z = L$ is accelerated by viscous, gravity, and capillary forces, Figure 1. Viscous forces dominate in melt spinning, which results in the momentum equation

$$\frac{d}{dz}\left(\frac{\tau_{zz} - \tau_{rr}}{u}\right) = 0 \tag{1}$$

where τ_{zz} and τ_{rr} are the axial and radial stress, respectively, and u is the axial velocity along the threadline in the z direction. To proceed, one needs a suitable constitutive equation that relates the difference in viscoelastic stresses, $\tau_{zz} - \tau_{rr}$, to the velocity u and velocity gradient du/dz.

The normal stress difference, $\tau_{zz} - \tau_{rr}$, in Eq. 1 is expressed in terms of the velocity and velocity gradient through the nonlinear integral constitutive equation

$$\underline{\underline{\tau}}(t) = \int_{-\infty}^{t} \sum_k \frac{\alpha_k}{\lambda_k} e^{-(t-t')/\lambda_k} \cdot \frac{\alpha}{(a-3) + \beta I_B + (1-\beta) II_B} [\underline{\underline{B}}_t(t') - \underline{\underline{I}}]\, dt' \tag{2}$$

For steady flows Eq. 2 transforms to a constitutive equation that

relates stress to location:

$$\underline{\underline{\tau}}(z) = \int_{-\infty}^{z} \sum_k \frac{\alpha_k}{\lambda_k} e^{-[(1/\lambda_k)\int_{z'}^{z}(dz'/u(z'))]} \cdot \frac{\alpha}{(a-3) + \beta I_{\underline{\underline{B}}} + (1-\beta) II_{\underline{\underline{B}}}} \cdot [\underline{\underline{B}}(z, z') - \underline{\underline{I}}] \frac{dz'}{u(z')} \quad (3)$$

The set $\{\alpha_k, \lambda_k\}$ consists of the common relaxation times and weights, α is a material parameter determined from shear tests, and β is a material parameter determined from elongational tests. $\underline{\underline{B}}(z, z')$ is the usual Finger tensor and I_B, II_B its first and second invariants. Further details are given elsewhere (Papanastasiou et al., 1983). The stress $\underline{\underline{\tau}}(z)$ on a liquid particle at z is a function of the relative deformation $\underline{\underline{B}}(z, z')$ to which the particle was exposed as it proceeded along its streamline $-\infty < z' < z$ from far away, Figure 2. The memory of the liquid fades with the ratios of transit time $t - t' = \int_{z'}^{z} dz/u(z)$ to the characteristic relaxation times λ_k.

The integral Eq. 3 involves an unbounded domain of integration. It is advantageous to break up that domain as shown in Figure 2. Within the first subdomain, which represents prehistory, the kinematics are assumed known up to an arbitrary constant, c, which is determined simultaneously with the solution within the second subdomain. The prehistory kinematics must satisfy the continuity of velocity and stress at the synthetic inlet at $z = 0$, for otherwise artificial stress and velocity boundary layers may be induced. A simple extensional prehistory $u(z) = \exp\{cz\}$ is a good approximation for long fibers. Demanding continuity of velocity and stress at the inlet permits the simultaneous evaluation of the prehistory parameter c and either the drawing force F or the draw ratio D_R with the evaluation of velocity distribution within the flow domain. The constitutive equation for an extensional prehistory in which the axial velocity is

$$v = e^{cz}, \quad 0 > z > -\infty, \quad (4)$$

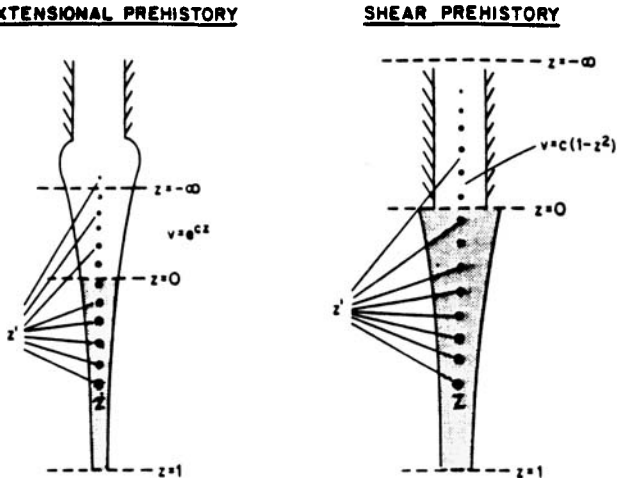

Figure 2. Flow domain ($0 \le z \le 1$) in modeling of fiber spinning with integral constitutive equations with prehistory ($-\infty < z \le 0$).

takes the form, Figure 2:

$$\underline{\underline{\tau}}(z) = \sum_k \frac{\alpha_k}{\lambda_k} \int_{-\infty}^{0} \exp\left[-\frac{\int_{z'}^{0} \frac{dz'}{v} + \int_{0}^{z} \frac{dz'}{u(z')}}{\lambda_k}\right] \cdot H(I_B, II_{\underline{\underline{B}}}) B[v, u(z)] \frac{dz'}{v} + \sum_k \frac{\alpha_k}{\lambda_k} \int_{0}^{z} \exp\left[-\frac{\int_{z'}^{z} \frac{dz'}{u(z')}}{\lambda_k}\right] \cdot H(I_B, II_B) \underline{\underline{B}}[u(z'), u(z)] \frac{dz'}{u(z')} \quad (5)$$

The exponential term in the first integral represents transit times between past states in the prehistory and the present:

$$t - t' = \int_{z'}^{z} \frac{dz}{u(z')} = \int_{z'}^{0} \frac{dz}{v} + \int_{0}^{z} \frac{dz}{u(z')} \quad (6)$$

The exponential term in the second integral represents transit times between past states in the flow domain and the present:

$$t - t' = \int_{z'}^{z} \frac{dz'}{u(z')} \quad (7)$$

To relate the viscoelastic stress difference $\tau_{zz} - \tau_{rr}$ in Eq. 1 to the velocity through Eq. 5 the Finger tensors $\underline{\underline{B}}[u(z), v]$ and $\underline{\underline{B}}[u(z), u(z')]$ must be expressed in terms of the velocity. To do so we solve the relative deformation gradient equations

$$u(z') \frac{\partial \underline{\underline{F}}(z, z')}{\partial z'} = \frac{\partial u(z')}{\partial z'} \underline{\underline{F}}(z, z') \quad (8a)$$

$$\underline{\underline{F}}(z', z') = \underline{\underline{I}} \quad (8b)$$

$$\underline{\underline{B}}(z, z') = \underline{\underline{F}}(z, z')^{-1} \cdot \underline{\underline{F}}(z, z')^{-T} \quad (8c)$$

which yield the components of the relative deformation Finger tensor between past positions z' in an extensional history and present position z:

$$\underline{\underline{B}}(z, z'): \quad 0 \le z' < z \qquad \begin{bmatrix} \left[\frac{u(z)}{u(z')}\right]^2 & 0 & 0 \\ 0 & \frac{u(z')}{u(z)} & 0 \\ 0 & 0 & \frac{u(z')}{u(z)} \end{bmatrix} \quad (9a)$$

From this the required Finger tensors in Eq. 5 are found to be

$$\underline{\underline{B}}[u(z), u(z')] = \underline{\underline{B}}(z, z') \quad (9b)$$

and (Petrie, 1979)

$$\underline{\underline{B}}[u(z), v] = \underline{\underline{F}}^{-1}(z, z' = 0) \underline{\underline{B}}(z = 0, z') \underline{\underline{F}}^{-T}(z, z' = 0): \quad (9c)$$

$$\begin{bmatrix} \left[\frac{e^{cz'}}{u(z)}\right]^{-2} & 0 & 0 \\ 0 & \left[\frac{u(z)}{e^{cz'}}\right]^{-1} & 0 \\ 0 & 0 & \left[\frac{u(z)}{e^{cz'}}\right]^{-1} \end{bmatrix} \tag{9d}$$

Were a shearing prehistory $v = c(1 - r^2)$ assumed, the components of the corresponding Finger tensor $\underline{\underline{B}}[u(z), v]$ would be

$$\underline{\underline{B}}[u(z), v]: \begin{bmatrix} \left[\frac{u(z)}{u(0)}\right]^2\left[1 + \left(\frac{v_r}{v} z'\right)^2\right] & -\left[\frac{u(z)}{u(0)}\right]^{1/2}\left(\frac{v_r}{v} z'\right) & 0 \\ -\left[\frac{u(z)}{u(0)}\right]^{1/2}\left(\frac{v_r}{v} z'\right) & \frac{u(0)}{u(z)} & 0 \\ 0 & 0 & \frac{u(0)}{u(z)} \end{bmatrix} \tag{9e}$$

At this stage, all dependent variables in Eq. 5 have been expressed in terms of past $u(z')$ and present $u(z)$ velocities. Thus Eq. 1 is an integrodifferential equation for the velocity distribution $u(z)$ and the unknown prehistory c.

At the inlet, the velocity and stresses calculated within the domain must match those predicted by the prehistory and thus

$$v(z = 0) = u(0) = 1 \tag{10a}$$

$$(\tau_{zz} - \tau_{rr})_{z=0^+} = (\tau_{zz} - \tau_{rr})_{z=0} \tag{10b}$$

At the outlet either the draw ratio

$$u(z = 1) = D_R \tag{11a}$$

or the drawing force

$$F = \left[\frac{\tau_{zz} - \tau_{rr}}{u(z)}\right]_{z=1} \tag{11b}$$

is specified.

The constitutive Eq. 2 reduces to an integral form that is equivalent to the upper-convected Maxwell model when $\alpha \to \infty$:

$$\underline{\underline{\tau}}(t) = \int_{-\infty}^{t} \sum_k \frac{\alpha_k}{\lambda_k} e^{-(t-t')/\lambda_k}[\underline{\underline{B}}_t(t') - \underline{\underline{I}}]\, dt' \tag{12}$$

If in addition $\lambda_k \to 0$, Eq. 12 reduces to the Newtonian constitutive law

$$\underline{\underline{\tau}}(t) = \int_{-\infty}^{t} \sum_k \frac{\alpha_k}{\lambda_k} e^{-(t-t')/\lambda_k}(t - t')\underline{\underline{D}}(t)\, dt$$

$$= \sum_k a_k\lambda_k\underline{\underline{D}}(t) = \mu\underline{\underline{D}}(t) \tag{13}$$

where μ is the zero shear viscosity and $\underline{\underline{D}}(t)$ is the rate of strain tensor. Thus the Maxwellian and the Newtonian solutions to Eq. 1 can be produced as limiting cases of the integral Eq. 5 by suitably choosing the material parameters λ_k and α.

Finite-element analysis

Equation 1 reduces to the integrodifferential equation

$$\frac{d}{dz}\left[\frac{1}{u(z)}(\tau_{zz} - \tau_{rr})\right] = 0 \tag{14}$$

where $\tau_{zz} - \tau_{rr}$ is given by Eq. 5 in terms of present, $u(z)$, and past, $u(z')$ and v, velocities. The unknown velocity is approximated by a set of quadratic basis functions

$$u(z) = \sum_1^N u_i\phi_i(z) \tag{15}$$

Then Eq. 14 is weighted integrally with these basis functions and the resulting weighted residuals, R_i, are required to vanish—Galerkin's method of weighted residuals. Applying the divergence theorem to the weighted residuals yields

$$\begin{aligned} R_i &= \left[\frac{\tau_{zz} - \tau_{rr}}{u(z)}\phi^i\right]_{z=1} - \left[\frac{\tau_{zz} - \tau_{rr}}{u(z)}\phi^i\right]_{z=0} \\ &\quad - \int_0^1 \frac{\tau_{zz} - \tau_{rr}}{u(z)}\frac{d\phi^i}{dz}\, dz \\ &= f - \left|\frac{\tau_{zz} - \tau_{rr}}{u(z)}\phi^i\right|_{z=0} - \int_0^1 \frac{\tau_{zz} - \tau_{rr}}{u(z)}\frac{d\phi}{dz}\, dz \\ &= f - \left(\frac{1}{u(z)}\left\{\int_{-\infty}^{0} G_1[c, u(o)]\, dz'\right\}\phi^i\right)_{z=0} \\ &\quad - \int_0^1 \frac{1}{u(z)}\left\{\left(\int_{-\infty}^{0} G_1[c, u(z'), u(z)]\, dz'\right.\right. \\ &\quad \left.\left. + \int_0^z G_2[u(z), u(z')]\, dz'\right\}\frac{d\phi^i}{dz}\, dz = 0 \end{aligned} \tag{16}$$

Here $f = FL/\mu Q$ is the dimensionless drawing force. The boundary residual R_1 at the inlet is replaced by the essential boundary condition $u(z = 0) = 1$ and thus

$$R_1 = 0 \tag{17}$$

The prehistory parameter c in the equation set is determined by requiring the traction to be continuous at the inlet:

$$R_{N+1} = f - \left[\frac{\tau_{zz} - \tau_{rr}}{u(z)}\right]_{z=0} = 0 \tag{18}$$

The system is closed by specifying either the draw ratio D_R or the drawing force f at the take-up end and thus

$$R_{N+2} = 0 \tag{19}$$

Equations 16–19 are a system of $N + 2$ nonlinear algebraic equations. To solve these equations we used full Newton iteration

$$\underline{u}^{(n+1)} = \underline{u}^{(n)} - \underline{\underline{J}}^{-1}\underline{R}(\underline{u}^{(n)}) \tag{20}$$

Here $\underline{u} = \{u_1, u_2 \ldots u_N = D_R, c, f\}$ is the matrix vector of the unknowns and $\underline{\underline{J}} = \partial \underline{R}/\partial \underline{u}$ is the Jacobian, a lower triangular matrix, the structure of which mirrors the fading memory of the viscoelastic liquid. In the matrix form $\underline{\underline{J}}[\underline{u}^{(n+1)} - \underline{u}^{(n)}] = -\underline{R}[\underline{u}^{(n)}]$,

$$
\begin{bmatrix}
1 & 0 & 0 & 0 & 0 & 0 & 0 & 0 & 0 & 0 & 0 & 0 \\
P & P & P & & & & & & & & S & 0 \\
M & P & P & P & & & & & & & S & 0 \\
M & M & P & P & P & & & & & & S & 0 \\
M & M & M & P & P & P & & & & & S & 0 \\
M & M & M & M & P & P & P & & & & S & 0 \\
M & M & M & M & M & P & P & P & & & S & 0 \\
0 & M & M & M & M & M & P & P & P & & S & 0 \\
0 & 0 & M & M & M & M & M & P & P & P & & 0 \\
0 & 0 & 0 & M & M & M & M & M & P & P & P & F \\
0 & 0 & 0 & 0 & M & M & M & M & M & P & P & F \\
0 & 0 & 0 & 0 & 0 & 0 & 0 & 0 & 0 & 0 & 1 & 0
\end{bmatrix}
\times
\begin{bmatrix}
u_1^{(n+1)} - u_1^{(n)} \\
u_2^{(n+1)} - u_2^{(n)} \\
\vdots \\
u_N^{(n+1)} - u_N^{(n)} \\
f^{(n+1)} - f^{(n)} \\
c^{(n+1)} - c^{(n)}
\end{bmatrix}
= -
\begin{bmatrix}
0 \\ R_2 \\ \vdots \\ R_N \\ R_{N+1} \\ 0
\end{bmatrix}
\tag{21}
$$

where

$M = \partial R/\partial u(z')$ = Sensitivity of stress with respect to upstream kinematics because of the memory of the liquid
$P = \partial R/\partial u(z)$ = Sensitivity of stress with respect to local kinematics
$S = \partial R/\partial c$ = Sensitivity of stress with respect to the kinematics in prehistory
$F = \partial R/\partial f$ = Sensitivity of stress with respect to the drawing force

Unity changes position in the last row, as shown in the matrix, depending on the desired boundary condition at the take-up end (draw ratio D_R or drawing force f).

Typical discretizations into elements are shown on the z axis of the figures with the results, e.g. figure 4. A fine tessellation was necessary near the matching inlet and near the take-up end where the extension rate is high. For all calculations the discretization was refined further and further until the solution became insensitive to additional refinement (changes in $\underline{R}$ less 10^{-6}).

The Newton iteration converges to a solution that yields the velocity distribution along the fiber $\{u_1 \ldots u_{n-1}\}$, the draw ratio $u_N = D_R$ or the drawing force f, and the prehistory parameter c. This prehistory parameter attains the value that guarantees a smooth, continuous transition from the upstream kinematics to those downstream within the finite-element domain.

Results and Discussion

The results are presented in terms of the following dimensionless numbers:

$$\text{Deborah number} \quad De = \dot{\epsilon}\frac{\Sigma\alpha_k\lambda_k^2}{\Sigma\alpha_k\lambda_k} = \dot{\epsilon}\bar{\lambda} \tag{22a}$$

$$\text{Relaxation number} \quad \lambda = \frac{u_o}{L}\cdot\frac{\Sigma\alpha_k\lambda_k^2}{\Sigma\alpha_k\lambda_k} = \frac{u_o}{L}\bar{\lambda} \tag{22b}$$

$$\text{Drawing force} \quad f = \frac{FL}{\mu Q} \tag{22c}$$

$$\text{Draw ratio} \quad D_R = \frac{u(z=1)}{u(z=0)} \tag{22d}$$

Here, $\dot{\epsilon} = (\partial u/\partial z)_{z=1}$ is the extension rate at the take-up end: $\mu = \Sigma\alpha_k\lambda_k$ is the zero shear viscosity; and $\bar{\lambda} = \Sigma\alpha_k\lambda_k^2/\Sigma\alpha_k\lambda_k$ is the average relaxation time. The other variables are shown in Figure 1.

Typical rates of convergence of Newton iteration are shown in Figure 3. Converged solutions are initial approximations to the solution at the higher Deborah number (zero-order continuation). In the limiting case of the upper-convected Maxwell model ($\alpha = 10{,}000$) the convergence was quadratic only at low Deborah numbers ($De < 1$). Near $De = 1$ the rate slowed and beyond $De = 1$ the Newton iteration never converged. This behavior is typical of the Newton iteration in the neighborhood of approaching an irregular point (singularity, turning, or bifurcation point). Indeed it is well known that the upper-convected Maxwell model predicts unbounded elongational stresses at $De = 1$ (Petrie, 1979). For the full nonlinear integral equation, quadratic convergence, as shown by Figure 3, was achieved up to Deborah number beyond 60.

By choosing a small relaxation time ($\lambda = 0.001$) and large shear material parameter ($\alpha = 10{,}000$) in the constitutive equation, the asymptotic Newtonian solution $u = \exp\{z \ln D_R\}$ was reproduced by the finite-element predictions as shown by Figure

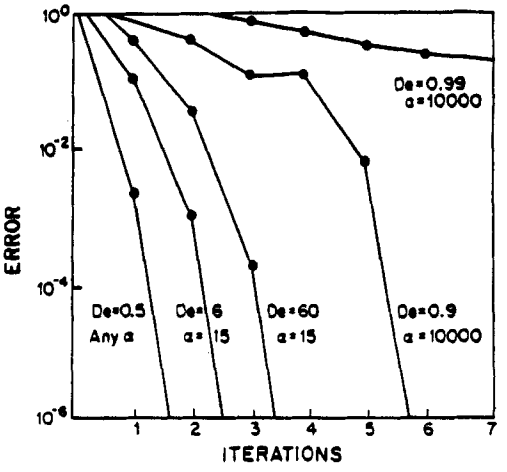

Figure 3. Rates of convergence of Newton iteration.
$\alpha = 15$, General nonlinear equation
$\alpha = 10{,}000$, Maxwell limiting case
Error defined as:
$\max\{|u_i^{(n+1)} - u_i^{(n)}|, |f^{(n+1)} - f^{(n)}|, |c^{(n+1)} - c^{(n)}|\}$

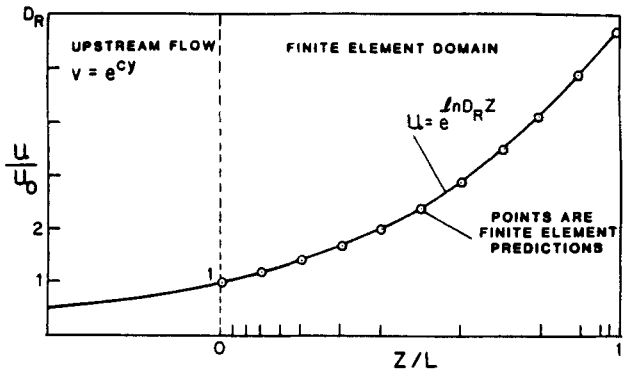

Figure 4. ○ ○ ○ Finite-element predictions with integral constitutive equation in limiting case (α = 10,000, λ = 0.001).

— Asymptotic solution for Newtonian liquids

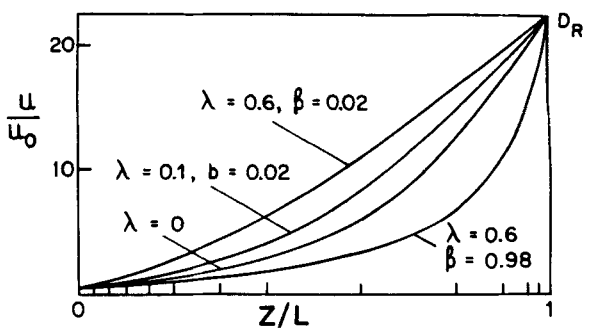

Figure 6. Finite-element predictions with nonlinear integral constitutive Eq. 15.

β = 0.98, Extension thinning liquid
λ = 0, Newtonian liquid
β = 0.02, Extension thickening liquid

4. Not only do the two solutions in the flow domain ($0 < z < 1$) agree to within 1% error, but the material parameter c in the prehistory region ($-\infty < z < 0$) attains the asymptotic value of the Newtonian solution $c = \ln D_R$ as well.

Finite-element predictions in the limiting case of the upper-convected Maxwell model (α = 10,000) are shown in Figure 5. For comparison, the results of Denn et al., (1975) obtained with the equivalent differential upper-convected Maxwell model are also shown there. The two solutions agree to within 0.5% at all elasticity levels. At λ = 0.052, at which the Deborah number $De = \lambda \dot{\epsilon}_{max} = \lambda(\partial u/\partial z)_{z=1}$ approached unity, both methods predicted a linear velocity profile. At this point the convergence rate slowed and beyond De = 1 the Newton iteration diverged.

In Figure 6 results with the full nonlinear integral model are shown for α = 10.5. Solutions were obtained at high Deborah numbers, $De > 100$. The behavior of the solution depended on the extensional material parameter β in the constitutive equation. For vanishingly small β (extension thickening) higher velocities and thus thinner fibers were obtained than in the Newtonian case (λ = 0). The opposite is true for β near unity (extension thinning).

The instantaneous elongational viscosity defined as

$$\eta_e = \frac{\tau_{zz} - \tau_{rr}}{\partial u/\partial z} \tag{23}$$

along the fiber in the three cases β = 0.02, λ = 0, and β = 0.98 of Figure 6 is plotted in Figure 7. As expected, the three distinct behaviors in extension are recovered: extension thickening for β = 0.02, Newtonian for $\lambda = 0$ and any β, and extension thinning for β = 0.98. Moreover, the three curves come together at low extension rates, and at $\epsilon \sim 10^{-2}$ s^{-1} all three cases exhibit the Trouton (1906) extensional viscosity, which is three times the zero shear viscosity. All three cases—thickening, Newtonian, and thinning—have been observed in experiments and reported in the literature (Ferguson and Missaghi, 1982).

The dimensionless force ($FL/\mu Q$) that is required to draw fibers of several elasticities ($\lambda u_o/L$) at a given draw ratio (D_R = 5.85) is plotted in Figure 8. Departing from the Newtonian limit ($\lambda u_o/L = 0$) it either increases or decreases with the elasticity of the liquid, depending again on the extensional material parameter β in the constitutive equation. In both cases, however, it is bounded and approaches a finite asymptotic value. For comparison, the predictions of Fisher and Denn (1976) with the upper-convected Maxwell model are also shown there: the predicted force becomes unbounded at moderate elasticity ($\lambda u_o/L$ = 0.6) where De = 1, and thus unbounded elongational stress is predicted by the upper-convected Maxwell model.

Comparison with Experiments

Here we compare our predictions to the data of Spearot and Metzner (1972) with a low-density polyethylene, and the data of

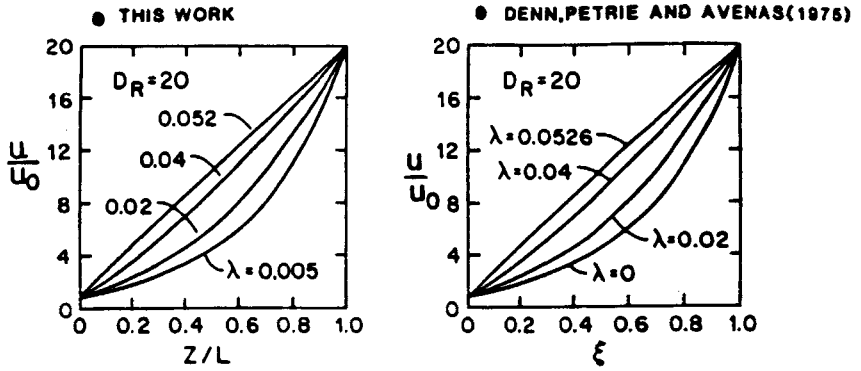

Figure 5. Left, finite-element predictions with integral constitutive equation in upper-convected Maxwell limiting case (α = 10,000).

Right, results of Denn et al. (1975) with equivalent differential upper-convected Maxwell model

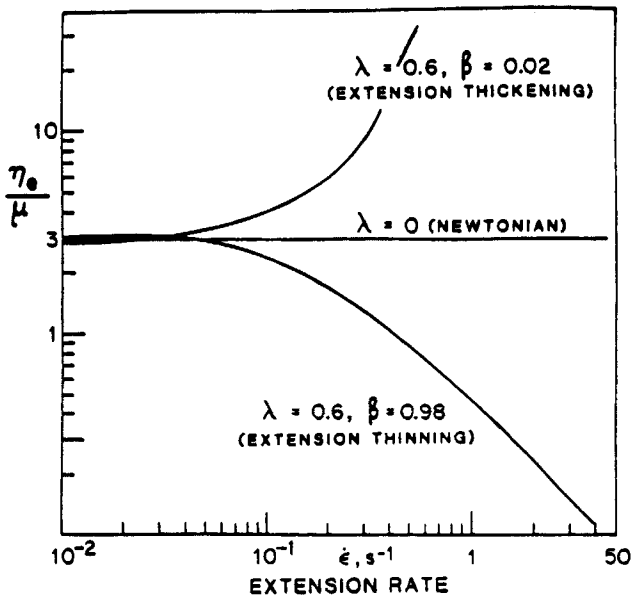

Figure 7. Calculated instantaneous extensional viscosity along fiber as a function of local extension rate.

Zeichner (1973) with polystyrene. These are the same data used by Phan-Thien (1978) to test his predictions. Unfortunately no specific rheological data at the spinning conditions were listed in any of these references. Thus we had to deduce these rheological data from other references, as Phan-Thien did.

The spinning conditions at $T = 170°C$ of polystyrene are shown in Table 1. To determine the relaxation spectrum we used the shear relaxation modulus at $T = 165°C$ given by Phan-Thien. The relaxation times λ_k, and the coefficients α_k were calculated by nonlinear regression analysis as in Papanastasiou et al. (1983). Then these relaxation times and coefficients were shifted to $T = 170°C$ by means of the WLF equation (Ferry, 1970). The resulting spectrum at $T = 170°C$ is shown in Table 2. The remaining material parameters, α and β, in the constitutive equation at $T = 170°C$ were taken from Papanastasiou et al. (1983) who used Laun's (1978) data. Their values are $\alpha = 10.57$ and $\beta = 0.022$. Figure 9 shows the predicted velocity distribu-

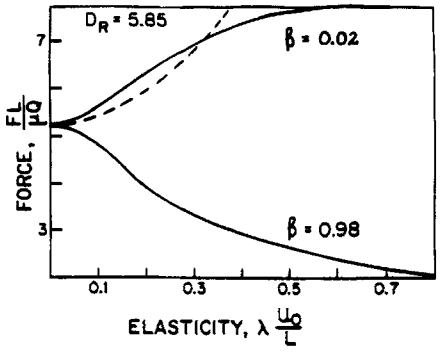

Figure 8. — Drawing forces computed by Eq. 5. --- Results of Fisher and Denn (1976) with upper-convected Maxwell model.

$\beta = 0.02$, Extension thickening liquid
$\beta = 0.98$, Extension thinning liquid

Table 1. Spinning Conditions of Polystyrene (Zeichner, 1973)

Temperature, $T = 170°C$
Velocity, $V = 0.0029$ m/s
Length, $L = 0.20$ m
Flow rate, $Q = 3.28 \times 10^{-5}$ kg/s
Drawing force, $F = 0.117$ N
Draw ratio, $D_R = 5.85$

Table 2. Relaxation Spectrum of Polystyrene at 170°C

λ_k s	α_k Pa
1.77E + 2	9.78E + 1
2.09E + 1	3.46E + 3
3.93E 0	6.78E + 3
4.39E − 1	1.01E + 4
5.05E − 2	1.26E + 4
7.55E − 3	1.45E + 4
4.55E − 4	1.47E + 4

Table 3. Spinning Conditions of Low-Density Polyethylene (Spearot and Metzner, 1972)

Temperature, $T = 150°C$
Velocity, $V = 0.009$ m/s
Length, $L = 0.30$ m
Flow rate, $Q = 1.15 \times 10^{-7}$ m³/s
Drawing force, $F = 0.111$ N
Draw ratio, $D_R = 2.61$

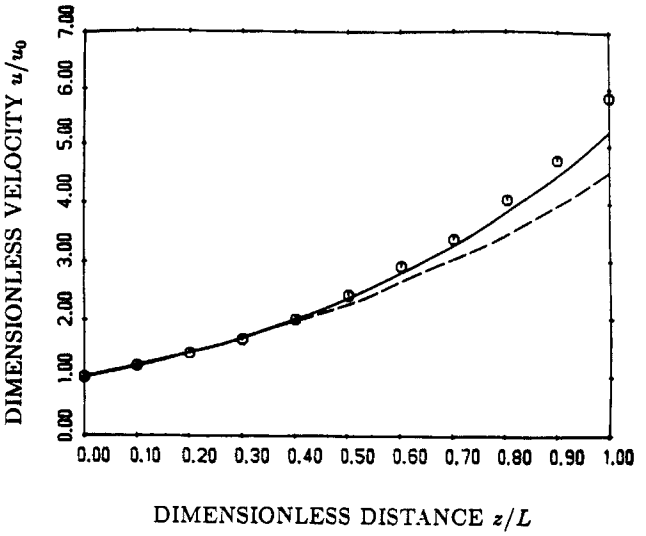

Figure 9. Velocity along fiber.

— Finite-element predictions, Eq. 15
O O O Data of Zeichner (1973)
--- Predictions of Phan-Thien (1978)
Experimental conditions and parameters listed in Tables 1 and 2

Table 4. Relaxation Spectrum of Low-Density Polyethylene at 150°C

λ_k s	α_k Pa
3.62E + 2	1.59E + 1
4.96E + 1	4.33E + 2
1.21E + 1	4.76E + 2
5.17E 0	2.57E + 3
4.94E − 1	7.61E + 3
5.48E − 2	1.45E + 4
8.40E − 3	2.29E + 4

tion compared with that measured by Zeichner; the predictions of Phan-Thien are also shown. Under drawing force $F = 0.117$ N the actual draw ratio at the take-up end was $D_R = 5.85$; Phan-Thien predicted $D_R = 4.66$, and we predicted $D_R = 5.46$.

The spinning conditions of low-density polyethylene are shown in Table 3. The relaxation times and coefficients were calculated by nonlinear regression analysis from the shear modulus given by Phan-Thien, and are shown in Table 4. The shear material parameter, α, was determined from the first normal stress difference given by Phan-Thien as $\alpha = 23$. For the extensional material parameter β, we used $\beta = 0.018$ of a similar polyethylene because the value of β was from 0.018 to 0.020 for all the melts examined (Papanastasiou et al., 1983). Figure 10 shows the predicted velocity distribution compared to that measured by Spearot and Metzner (1972) and to that predicted by Phan-Thien (1978). Under drawing force $F = 0.111$ N the actual draw ratio was $D_R = 2.61$; Phan-Thien predicted $D_R = 2.55$, and we predicted $D_R = 2.78$.

We solved the same problems with a draw ratio boundary condition. We found that in order to spin the polystyrene at draw ratio $D_R = 5.85$ a drawing force $F = 0.126$ N is required. This value differs by 7.3% from that measured in Table 1. To spin the low-density polyethylene at draw ratio $D_R = 2.61$ a drawing force $F = 0.10401$ N was calculated. This value differs by 6.4% from that measured in Table 3. No comparisons to the results of Phan-Thien have been made because he analyzed the flow with a drawing force boundary condition alone.

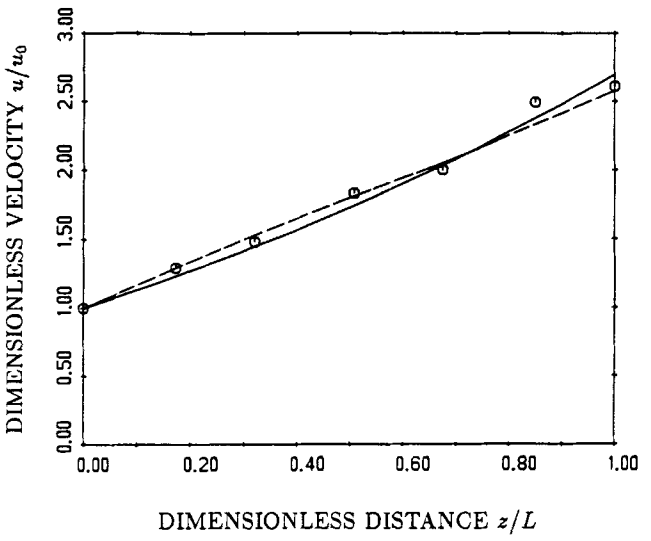

Figure 10. Velocity along fiber.
— Finite-element predictions, Eq. 15
O O O Data of Spearot and Metzner (1972)
--- Predictions of Phan-Thien (1978)
Experimental conditions and parameters listed in Tables 3 and 4

Given the many sources of information used to determine the material parameters in the constitutive equation, it appears that both analyses, ours and that of Phan-Thien, account at least qualitatively for the viscoelastic responses in fiber spinning. We feel that our analysis is more general regarding the specifications at the take-up end, e.g., draw ratio or drawing force, and the significance of the prehistory of deformation. In addition, the integral constitutive equation is better suited for viscoelastic liquid and can represent the most sophisticated equations derived recently from molecular theories. The accuracy of the constitutive equation was tested in many kinds of controlled transient and steady deformation in shear, uniaxial elongation, and biaxial extension (Papanastasiou et al., 1983, 1984). The advantage of the Phan-Thien analysis is its simplicity compared to analyses with integral constitutive equations. This advantage, although critical in computations with two- and three-dimensional viscoelastic flows, is of minor significance in the one-dimensional fiber spinning process analyzed in this work.

Conclusions

Accurate constitutive equations, including those derived recently from the molecular theory of fluids, can be employed to study fiber spinning and related extrusion processes. The application is made possible by means of Galerkin finite-element discretization and Newton iteration. Such analysis showed that:

1. Integral constitutive equations are well suited for analyzing the fiber-spinning process because they can account for extension thinning and extension thickening, spectrum of relaxation times, history effects, and specified fiber diameter or applied tension.

2. The operating conditions depend largely on the extensional behavior of the viscoelastic liquid: extension thinning liquids yield thin fibers drawn by small forces, whereas the opposite is true for extension thickening liquids.

High extension rates were calculated (and also observed in experiments in the literature) in the fiber spinning process. In that respect the process would make an excellent rheometer. However, the achieved extensional deformation is history-dependent and inhomogeneous, and so data reduction independent of a constitutive equation is impossible. Thus the algorithm developed here and based on integral constitutive equations may prove essential in data reduction with commercially available fiber-spinning rheometers.

Notation

$\underline{\underline{B}}$ = Finger deformation tensor
$\underline{\underline{D}}$ = rate of strain tensor
$\overline{D}$ = diameter of fiber
D_R = draw ratio
F = drawing force
$\underline{\underline{F}}$ = deformation gradient tensor
$\bar{f}$ = dimensionless drawing force
g = acceleration of gravity
$\underline{\underline{I}}$ = unit tensor
$\overline{L}$ = length of fiber
p = pressure within fiber
Q = volumetric flow rate
R = radius of fiber
t = time
u = axial velocity along fiber

u_o = axial velocity at inlet
u_L = axial velocity at take-up end
v = axial velocity prior to inlet
z = axial distance along fiber

Greek letters

α = shear material parameter
α_k = relaxation coefficient
β = extensional material parameter
η_e = elongational viscosity
$\dot{\epsilon}$ = extension rate, $\partial u/\partial z$
$\bar{\lambda}$ = average relaxation time
λ = dimensionless average relaxation time
λ_k = relaxation time
μ = dynamic viscosity
π = 3.14
ρ = density
σ = surface tension
$\underline{\tau}$ = stress tensor
τ_{zz} = axial stress
τ_{rr} = radial stress
ϕ_i = finite-element basis function

Literature cited

Bernstein, B., E. A. Kearsley, and L. J. Zapas, "A Study of Stress Relaxation with Finite Strain," *Trans. Soc. Rheol.*, **7**, 391 (1963).

Curtiss, C. F., and R. B. Bird, "A Kinetic Theory for Polymer Melts. II The Stress Tensor and the Rheological Equation of State," *J. of Chem. Phys.*, **74**, 2026 (1981).

Denn, M. M., C. J. S. Petrie, and P. Avenas, "Mechanics of Steady Spinning of a Viscoelastic Liquid," *AIChE J.*, **21**, 791 (1975).

Doi, M., and S. F. Edwards, "Dynamics of Rod-like Macromolecules in Concentrated Solutions," *J. Chem. Soc. Faraday Trans.*, **74**, 918 (1979).

Ferguson, J., and K. Missaghi, "Viscous and Elastic Effects in Extensional Flow," *J. Non-Newt. Fluid Mech.*, **11**, 269 (1982).

Ferry, J. D., *Viscoelastic Properties of Polymers*, Wiley, New York (1970).

Fisher, R. J., and M. M. Denn, "A Theory of Isothermal Melt Spinning and Draw Resonance," *AIChE J.*, **22**, 236 (1976).

Keunings, R., M. J. Crochet, and M. M. Denn, "Profile Development in Continuous Drawing of Viscoelastic Liquids," *Ind. Eng. Chem. Fundam.*, **22**, 347 (1983).

Larson, R. G., "Analysis of Isothermal Fiber Spinning with the Doi-Edwards Constitutive Equation," *J. Rheol.*, **27**, 475 (1983).

Laun, H. M., "Description of the Nonlinear Shear Behavior of a Low-Density Polyethylene Melt by Means of an Experimentally Determined Strain-Dependent Memory Function," *Rheol. Acta.*, **17**, 1 (1978).

Lodge, A. S., "Stress Relaxation after a Sudden Shear Strain," *Rheol. Acta*, **14**, 664 (1975).

Malkus, D. S., "Functioning Derivatives and Finite Elements for the Steady Spinning of a Viscoelastic Filament," *J. Non-Newt. Fluid Mech.*, **8**, 223 (1981).

Matovich, M. A., and J. R. A. Pearson, "Spinning a Molten Threadline," *Ind. Eng. Chem. Fundam.*, **8**, 512 (1969).

Mewis, J., and G. D. Gleyn, "Shear History Effects in the Spinning of Polymers," *AIChE J.*, **28**, 900 (1982).

Papanastasiou, T. C., L. E. Scriven, and C. W. Macosko, "An Integral Constitutive Equation for Mixed Flows: Viscoelastic Characterization," *J. Rheol.*, **27**, 387 (1983).

———, "Bubble Growth and Collapse in Viscoelastic Liquids Analyzed," *J. Non-Newt. Fluid Mech.*, **16**, 53 (1984).

Petrie, C. J. S., *Elongational Flows*, Pitman, London (1979).

Phan-Thien, N., "A Nonlinear Network Viscoelastic Model," *J. Rheol.*, **22**, 259 (1978).

Phan-Thien, N., and R. I. Tanner, "A New Constitutive Equation Derived from Network Theory," *J. Non-Newt. Fluid Mech.*, **2**, 353 (1977).

Spearot, J. A., and A. B. Metzner, "Isothermal Spinning of Molten Polyethylenes," *Trans. Soc. Rheol.*, **16**, 495 (1972).

Trouton, F. T., "On the Coefficient of Viscous Traction and Its Relation to that of Viscosity," *Proc. Roy. Soc.*, **A77**, 426 (1906).

Zeichner, G. R., "Spinnability of Viscoelastic Fluids," M.Ch.E. Thesis, Univ. Delaware (1973).

Manuscript received Mar. 28, 1986, and revision received Oct. 20, 1986.

Correction

In the paper titled "Separation Synthesis of Multicomponent Feed Streams into Multicomponent Product Streams" (April 1987, p. 547), we published Figure 7 with wrong numbers. Here is the updated figure.